Front. Phys. China, 2007, 2(4): 389−402
DOI 10.1007/s11467-007-0061-0

RESEARCH ARTICLE

TONG Zhao-yang, LIAO Ping, KUANG Le-man

Quantum repeaters based on CNOT gate under decoherence

© Higher Education Press and Springer-Verlag 2007

Abstract In this paper, we study single-qubit and single-user quantum repeaters based on CNOT gates under decoherence using the Kraus-operator representations of decoherence. We investigate the influence of decoherence on the information-disturbance trade-off of quantum repeaters. It is found that decoherence may lead to the appearance of three subspaces, called as the normal subspace, the anomalous subspace, and the decoherence-free subspace (DFS), respectively. It is indicated that in the normal subspace decoherence decreases the transmission and estimation fidelities, in the anomalous subspace decoherence enhances these fidelities, and in the DFS these fidelities do not change. The concept of the quality factor is introduced to evaluate the quality of the quantum repeater. It is indicated that the quality factor can be efficiently controlled and manipulated by changing the initial state of the probe qubit. It is found that under certain conditions the quantum repeater can be optimal even in the presence of decoherence.

Keywords quantum repeaters, quantum decoherence, quality factor, information-disturbance tradeoff, Kraus operators

PACS numbers 03.67.Hk, 03.65.Ud, 03.67.Lx

1 Introduction

In recent years, much attention has been paid to quantum repeaters [1–15] which permit the retrieval of information without the destruction of the carrier. Actually, the extracting process of information in a quantum repeater can be expressed in terms of a series of quantum measurement processes upon the information carrier and the probe system. As well known, any kind of measurements performed on a quantum system [16–25] will inevitably alters the quantum system itself. As a general rule, the more information obtained from a quantum state of the carrier, the higher the disturbance applied to the state. The trade-off between the amounts of the extracted information about a quantum state and the corresponding added disturbance is one of fundamental problems in quantum mechanics and is of practical applications in quantum communication [26–30]. In particular, the quantum-state disturbance caused by the information gain has become an issue of practical significance since it underlies the security of quantum key distribution and quantum cryptography [31–35].

The trade-off between information gain and quantum state disturbances can be quantified using two fidelities [36–45], which may be defined as follows. Suppose now you have a quantum system in a pure state $|\psi\rangle$ If the outcome k is observed at the output of the quantum repeater, then the estimated signal state is given by $|\phi_k\rangle$ (the typical inference rule being $k \to |\phi_k\rangle$ with $|\phi_k\rangle$ given by the set of eigenstates of the measured observable), whereas the conditional state of the second output $|\psi_k\rangle$ is left to the subsequent user. The amount of state disturbance is quantified by evaluating the overlap of the conditional state $|\psi_k\rangle$ to the initial one $|\psi\rangle$, whereas the amount of information extracted by the measurement corresponds to the overlap of the inferred state $|\phi_k\rangle$ to the initial one. The corresponding fidelities, for a given input signal $|\psi\rangle$, are given by

$$F_\psi = \sum_k P_k |\langle\psi|\psi_k\rangle|^2, \quad G_\psi = \sum_k P_k |\langle\psi|\phi_k\rangle|^2 \tag{1}$$

TONG Zhao-yang, LIAO Ping, KUANG Le-man (✉)
Key Laboratory of Quantum Structures and Quantum Control of Ministry of Education, and Department of Physics, Hunan Normal University, Changsha 410081, China
E-mail: lmkuang@hunnu.edu.cn

Received August 25, 2007

where we have already performed the average over the distribution P_k of the outcomes. The relevant quantities to assess the quantum repeater are then given by the average fidelities

$$F = \int_A \mathrm{d}\psi F_\psi, \quad G = \int_A \mathrm{d}\psi G_\psi \tag{2}$$

which are obtained by averaging F_ψ and G_ψ over all of the possible input states, i.e., over the alphabet A of the transmittable symbols. F will be referred to as the transmission fidelity, which describes how much the state after the operation resembles the original one. G will be referred as the estimation fidelity, which characterizes the average quality of our guess. Of course we have $0 \leqslant G \leqslant 1$ and $0 \leqslant F \leqslant 1$ with $F = 1$ corresponding to zero disturbance and $G = 1$ to complete information.

The two fidelities F and G are not independent of each other. Banaszek [36] has explicitly derived the information trade-off bound. For randomly distributed qubits with the alphabet A equal to the whole Bloch sphere, the information-disturbance trade-off satisfies the following inequality

$$\left(F - \frac{2}{3}\right)^2 + 4\left(G - \frac{1}{2}\right)^2 \leqslant \frac{1}{9} \tag{3}$$

From Eq.(3), one knows the maximum transmission fidelity compatible with a given value of the estimation fidelity or, in other words, the minimum unavoidable amount of noise that is added to the knowledge about a set of signals if one wants to achieve a given level of information.

In order to evaluate the optimal character of a quantum repeater, we introduce a quality factor defined by

$$Q = 9\left(F - \frac{2}{3}\right)^2 + 36\left(G - \frac{1}{2}\right)^2 \tag{4}$$

From the inequality of the information-disturbance trade-off given by Eq.(3) we can see that the quality factor is generally less than unity and an optimal quantum repeater has $Q = 1$.

On the other hand, a crucial obstruction to the realization of quantum information processing devices (QIPD) is decoherence which is caused by the unwanted interaction of the system with its environment [46−49]. Quantum systems are generally very fragile to decoherence which can suppress various nonclassical effects of quantum systems [50−55]. Even for the simple special purpose quantum devices such as quantum repeaters, decoherence must be taken into account since very long quantum information storage times are required in these devices. A number of concepts have been developed to fight decoherence and increase the reliability of QIPD including active error correction [56−58] and fault tolerant quantum computing [59−62]. It has been shown that there may exist subspaces of the system's Hilbert space which are immune to decoherence processes induced by these unwanted interactions. These decoherence-free subspaces (DFS) [63−68] are a method of passive error correction or error prevention and can significantly increase the lifetime of quantum information and reliability of QIPD as already demonstrated with ion traps, NMR and optical methods. Recently, Genoni and Paris (GP) [69,70] have suggested a class of quantum repeaters based on CNOT-gate operations. The GP quantum repeaters are optimal since their transmission and estimation fidelities saturate the ultimate bound imposed by quantum mechanics. For a GP quantum repeater, neither the carrier system nor the probe system of quantum information can avoid decoherence induced by their environment. Thus, it is interesting and important to analyze effects of decoherence in real practical situations for finding out if GP quantum repeaters can maintain their optimality in the presence of decoherence and the DFS of the probe systems. The purpose of this paper is to investigate the influence of decoherence on the GP quantum repeaters with the single-signal qubit and the single-probe qubit and to explore the DFS of realizing quantum information extraction in the presence of decoherence. This paper is organized as follows. In Section 2, we present a brief review for GP quantum repeaters without decoherence. In Section 3, we describe the Kraus-operator representations of decoherence. Three kinds of typical damping channels, i.e., depolarizing channel, phase-damping channel, and amplitude-damping channel, are discussed in detail. In Section 4, we calculate the transmission fidelity and the estimation fidelity, analyze the trade-off between information gain and quantum state disturbances, and indicate the existence of the DFS. We shall conclude our paper with discussions and remarks in the last section.

2 A brief review for quantum repeaters without decoherence

In this section we present a brief review for quantum repeaters without decoherence [69] for the use in the next sections. The simplest single-qubit quantum repeater with one user is a four-port structure which is indicated in Fig.1. It consists of the carrier qubit, the probe qubit, the probe-qubit detector, and the CNOT gate which establishes the interaction between the carrier qubit and the probe qubit. Quantum information is encoded in a quantum state of the signal (carrier) qubit denoted by

$$|\Psi\rangle = \cos\theta_1|0\rangle + \mathrm{e}^{\mathrm{i}\phi_1}\sin\theta_1|1\rangle \tag{5}$$

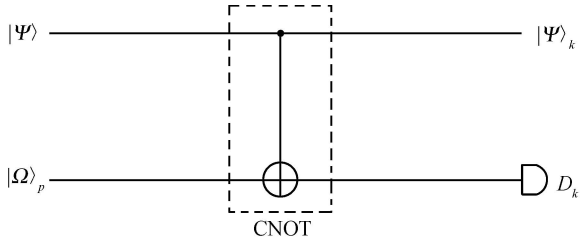

Fig. 1 Minimal implementation of an optimal single-qubit quantum repeater with one user without decoherence.

Suppose that the probe qubit is initially in the following state

$$|\Omega\rangle_p = \cos\theta_2|0\rangle_p + \mathrm{e}^{\mathrm{i}\phi_2}\sin\theta_2|1\rangle_p \tag{6}$$

The interaction between the signal qubit and the probe qubit can be realized through the CNOT gate where the signal qubit is the control qubit while the probe qubit is target qubit. Output states of the probe qubit depend on the probe-qubit detector D_k which carries out $\hat{\sigma}_z$ measurements upon the probe qubit. If after a $\hat{\sigma}_z$ measurement the probe qubit is in the state $|0\rangle$ (or $|1\rangle$) with the probability p_0 (or p_1), the amount of information extracted by the measurement corresponds to the overlap of the inferred state $|0\rangle$ (or $|1\rangle$) with respect to the initial state of the signal qubit

$$G_\Psi = P_0|\langle\Psi|0\rangle|^2 + P_1|\langle\Psi|1\rangle|^2 \tag{7}$$

The output states of the signal qubit can be obtained through the action of effective measurement operators induced by the CNOT gate operation on the input state of the signal qubit. Corresponding to the output states of the $\hat{\sigma}_z$ measurements for the probe qubit $|0\rangle$ and $|1\rangle$, the output states of the signal qubit are given by

$$|\Psi_0\rangle = \frac{1}{\sqrt{P_0}}A_0|\Psi\rangle, \quad |\Psi_1\rangle = \frac{1}{\sqrt{P_1}}A_1|\Psi\rangle \tag{8}$$

where the two effective measurement operators are given by

$$A_0 = \begin{pmatrix} \cos\theta_2 & 0 \\ 0 & \mathrm{e}^{\mathrm{i}\phi_2}\sin\theta_2 \end{pmatrix}$$
$$A_1 = \begin{pmatrix} \mathrm{e}^{\mathrm{i}\phi_2}\sin\theta_2 & 0 \\ 0 & \cos\theta_2 \end{pmatrix} \tag{9}$$

which indicate that the parameters in the two effective measurement operators are those of the initial state of the probe qubit. Hence, one can design effective measurement operators through a suitable preparation of the probe state.

The amount of disturbance of the signal state can be quantified through the mean fidelity, which is defined by the overlap of the conditional states $|\Psi_0\rangle$ and $|\Psi_1\rangle$ with respect to the initial state $|\Psi\rangle$:

$$F_\Psi = P_0|\langle\Psi|\Psi_0\rangle|^2 + P_1|\langle\Psi|\Psi_1\rangle|^2 \tag{10}$$

The mean fidelities F and G of the quantum repeater i.e., the transmission and estimation fidelities, are obtained by averaging over all the possible input states with the following expressions:

$$F_0 = \frac{1}{2\pi}\int_0^{2\pi}\mathrm{d}\phi_1\int_0^{\pi/2}\mathrm{d}\theta_1\sin(2\theta_1)\,F_\Psi$$
$$G_0 = \frac{1}{2\pi}\int_0^{2\pi}\mathrm{d}\phi_1\int_0^{\pi/2}\mathrm{d}\theta_1\sin(2\theta_1)G_\Psi \tag{11}$$

For the initial state of the probe qubit given by Eq. (6), through simple calculations one can obtain the two fidelities

$$F_0 = \frac{2}{3}\left[1+\frac{1}{2}\sin(2\theta_2)\cos\phi_2\right]$$
$$G_0 = \frac{1}{6}[3+\cos(2\theta_2)] \tag{12}$$

which implies that the transmission and estimation fidelities of the GP quantum repeater depend on the initial state of the probe qubit, and any allowed ration between the two fidelities may be achieved by tuning the initial-state parameters of the probe qubit.

Substituting Eq. (12) into Eq. (4) we find the quality factor of the GP quantum repeater in the absence of decoherence to be

$$Q_0 = 1-\sin^2(2\theta_2)\sin^2\phi_2 \tag{13}$$

which indicates that the optimality of the GP quantum repeater depends on the amplitude and phase parameters of the initial probe qubit θ_2 and ϕ_2. In particular, when $\phi_2 = k\pi$ or $\theta_2 = k\pi/2$ with k being an integer, we have $Q_0 = 1$ which implies the repeater is an optimal repeater for an arbitrary initial probe-qubit state with the phase $\phi_2 = k\pi$ or $\theta_2 = k\pi/2$.

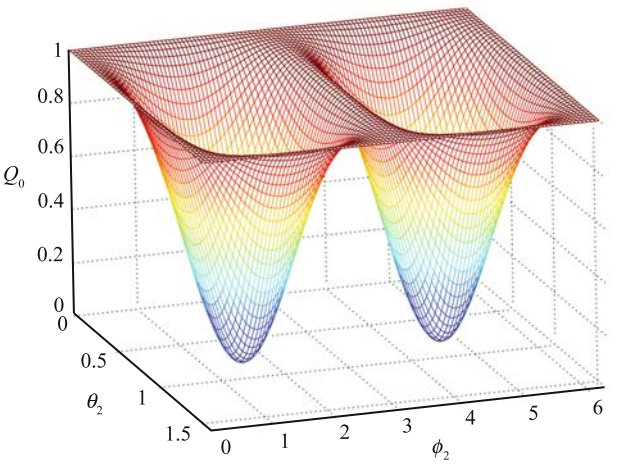

Fig. 2 The quality factor versus the amplitude and phase parameters of the initial probe qubit θ_2 and ϕ_2.

When $\theta_2 = (2r+1)\pi/4$ and $\phi_2 = (2s+1)\pi/2$ with r and s being integers, we have $Q_0 = 0$ which implies the repeater with the worst quality. To see the dependence of the quality factor on the initial probe qubit, we have plotted the quality factor versus the amplitude and phase parameters of the initial probe qubit θ_2 and ϕ_2 in Fig.2.

3 The Kraus-operator representations of decoherence

In this section, we describe the Kraus-operator representations of decoherence. Three kinds of typical damping channels, i.e., depolarizing channel, phase-damping channel, and amplitude-damping channel, are discussed in detail. In practice, it is a complicated problem to understand the environment effect on the quantum system. In general, there are three ideal models of noise to describe the environment effect [71, 72], called the amplitude damping, the phase damping, and the depolarizing channel, respectively. The amplitude and phase damping capture many of the most important features of the environment noise occurring in quantum mechanical systems. In order to understand the physical origin of them, let us briefly recall a few basic facts about the interaction between a quantum system and its environment. On one hand, one of the most important reasons for the quantum state change is the energy dissipation of the system induced by the environment. This energy dissipation can be characterized by the amplitude damping model. On the other hand, a state can be a superposition of different states, which is one of the main characteristics of the quantum mechanics. The relative phase and amplitude of the superposed state determines the properties of the whole state. If the relative phases of the superposed states randomly change with the time evolution, then the coherence of the quantum state will be destroyed. This kind of quantum noise process is called the phase damping. In this case, the energy eigenstates of a quantum system do not change as a function of time, but do accumulate a phase which is proportional to the eigenvalue. When the system evolves for an amount of time, partial information about the relative phases between energy eigenstates is lost.

The amplitude and phase damping can be mathematically described by decaying of the diagonal and off-diagonal elements of the reduced density operator of the system. The two effects can be understood in terms of Hamiltonian formalism. If we assume the total Hamiltonian of the system plus environment to be $H_T = H_S + H_R + H_I$, where H_S and H_R are Hamiltonians of the system and environment, respectively, and H_I is the interaction Hamiltonian between them. When the Hamiltonian of the system commutes with that of the interaction between the system and environment, i.e., $[H_S, H_I] = 0$, which means that there is no energy transfer between the system and the environment, energy of the system is conservative, so that what interaction between the system and environment describes is the phase damping effect. When $[H_S, H_I] \neq 0$, there is energy transfer between the system and environment, so that what interaction between the system and environment describes is the amplitude damping effect.

As is well known, the evolution of quantum states in the noisy environment can be well described in terms of Kraus operators [71−76]. The quantum system of the initial state $\rho_{\rm in}$ evolves to the final state $\rho_{\rm out}$ under the action of the noisy environment. One can related the initial state and the final state through using a superoperator $\rho_{\rm out} = \mathcal{S}(\rho_{\rm in})$ in which the quantum operation $\mathcal{S}$ on the state $\rho_{\rm in}$ can be described by the Kraus operator sum formalism as

$$\rho_{\rm out} = \sum_{\mu} M_\mu(p)\rho_{\rm in}M_\mu^\dagger(p) \tag{14}$$

where p is a parameter to describe the damping produced by the noise environment and it takes its values in the regime of $(0, 1)$. We have $p = 0$ in the absence of the damping while we have $p = 1$ the evolution time approaches the infinity. The two-bit Kraus operators $M_\mu(p)$ and $M_\mu^\dagger(p)$ act on the Hilbert space of the quantum system under consideration, they can be expressed in terms of single-qubit Kraus operators defined below and satisfy the completeness relation $\sum_\mu M_\mu^\dagger(p)M_\mu(p) = 1$.

These superoperators which can be expressed in terms of the Kraus operators are called as quantum channels. In what follows we describe three kinds of typical quantum channels, i.e., depolarizing channel, phase-damping channel, and amplitude-damping channel.

3.1 The depolarizing channel

In the depolarizing channel for a decohering qubit there are three types of errors which are called bit flip error $|0\rangle \to |1\rangle$ and $|1\rangle \to |0\rangle$, phase flip error, $|0\rangle \to |0\rangle$ and $|1\rangle \to -|1\rangle$, and bit-phase flip error $|0\rangle \to \mathrm{i}|1\rangle$ and $|1\rangle \to -\mathrm{i}|1\rangle$, respectively. The depolarizing channel has particularly nice symmetry properties. If an error happens with probability p, the qubit remains intact with probability $1 - p$. The error can be of any one of above three types where each type of errors is equally likely. These three types of errors can be expressed in terms of Pauli matrices as follows:

$$|\psi\rangle \to \hat{\sigma}_x|\psi\rangle, \quad |\psi\rangle \to \hat{\sigma}_z|\psi\rangle, \quad |\psi\rangle \to \hat{\sigma}_y|\psi\rangle \tag{15}$$

where for $|\psi\rangle$ is an arbitrary state of the qubit, $\hat{\sigma}_x$, $\hat{\sigma}_y$, and $\hat{\sigma}_z$ are Pauli matrices. If an error occurs, then $|\psi\rangle$ evolves to an ensemble of the three states $\hat{\sigma}_x|\psi\rangle$, $\hat{\sigma}_y|\psi\rangle$, and $\hat{\sigma}_z|\psi\rangle$, and all occurring with equal likelihood.

The depolarizing channel can be represented by a unitary operator $\hat{U}_{SE}$ acting on the total space of the qubit plus its environment with dimension 4. Suppose that before the errors occur, the total state of the qubit plus environment is $|\psi\rangle_S \otimes |0\rangle_E$. Then after the errors occurs, the total state of the qubit plus environment $\hat{U}_{SE}|\psi\rangle_S \otimes |0\rangle_E$ becomes

$$\begin{aligned}&\sqrt{1-p}|\psi\rangle_S \otimes |0\rangle_E + \sqrt{\frac{p}{3}}[\hat{\sigma}_x|\psi\rangle_S \otimes |1\rangle_E \\ &+\hat{\sigma}_y|\psi\rangle_S \otimes |2\rangle_E + \hat{\sigma}_z|\psi\rangle_S \otimes |3\rangle_E]\end{aligned} \tag{16}$$

where $\{|0\rangle_E, |1\rangle_E, |2\rangle_E, |3\rangle_E\}$ is an orthonormal basis for the environment. The Kraus operators of the depolarizing channel can be obtained through evaluating the partial trace over the environment in the $\{|i\rangle_E\}$ basis $M_i =_E \langle i|\hat{U}_{SE}|0\rangle_E$ with the following expressions

$$\begin{aligned}&M_0(p)=\sqrt{1-p}\begin{pmatrix}1&0\\0&1\end{pmatrix},\ M_1(p)=\sqrt{\frac{p}{3}}\begin{pmatrix}0&1\\1&0\end{pmatrix}\\ &M_2(p)=\sqrt{\frac{p}{3}}\begin{pmatrix}0&-\mathrm{i}\\\mathrm{i}&0\end{pmatrix},\ M_3(p)=\sqrt{\frac{p}{3}}\begin{pmatrix}1&0\\0&-1\end{pmatrix}\end{aligned} \tag{17}$$

which satisfy the normalization condition $\Sigma_{i=0}^{3} M_i = 1$. Therefore, in the depolarizing channel a general initial density matrix ρ of the qubit evolves as

$$\rho_{\mathrm{in}}^{'}=\begin{pmatrix}\left(1-\frac{2}{3}p\right)\rho_{00}+\frac{2}{3}p\rho_{11} & \left(1-\frac{4}{3}p\right)\rho_{01}\\ \left(1-\frac{4}{3}p\right)\rho_{10} & \left(1-\frac{2}{3}p\right)\rho_{11}+\frac{2}{3}p\rho_{00}\end{pmatrix} \tag{18}$$

which implies to sum over the four ways that the environment could evolve.

In order to intuitively understand the depolarizing channel, let us see how the depolarizing channel acts on the Bloch sphere. An arbitrary density matrix for a single qubit can be written as the following Bloch-sphere representation

$$\begin{aligned}\rho&=\frac{1}{2}\left(1+P\cdot\hat{\sigma}\right)\\ &=\frac{1}{2}\begin{pmatrix}1+P_3 & P_1-\mathrm{i}P_2\\ P_1+\mathrm{i}P_2 & 1+P_3\end{pmatrix}\end{aligned} \tag{19}$$

where $P = (P_x, P_y, P_z)$ is the "spin polarization" of the qubit.

It is straightforward to show that the evolution of the density operator of the qubit in the depolarizing channel (16) can be expressed as

$$\begin{aligned}&\rho' = \frac{1}{2}\left(1+P'\cdot\hat{\sigma}\right)\\ &P'_x=(1-4p/3)P_x,\quad P'_y=(1-4p/3)P_y\\ &P'_z=(1-4p/3)P_z\end{aligned} \tag{20}$$

where $P' = (P'_x, P'_y, P'_z)$ is the "spin polarization vector" of the qubit in the depolarizing channel given by

$$P' = \left(1-\frac{4}{3}p\right)P \tag{21}$$

which indicates that the Bloch sphere contracts uniformly under the action of the depolarizing channel while the direction of the spin polarization in which P points is independent of the damping, and the spin polarization length $|P|$ is reduced by the factor $1-4p/3$. This is the reason that this damping channel is called as the depolarizing channel.

3.2 The phase-damping channel

In the depolarizing channel, the decohering qubit does not make any transitions. Instead, the environment "scatters" off of the qubit occasionally (with probability p) being kicked into the state $|1\rangle_E$ if the qubit is in the state $|0\rangle_S$ and into the state $|2\rangle_E$ if the qubit is in the state $|1\rangle_S$. A unitary representation of the channel is given by

$$\begin{aligned}&|0\rangle_S|0\rangle_E \to \sqrt{1-p}|0\rangle_S|0\rangle_E + \sqrt{p}|0\rangle_S|1\rangle_E\\ &|1\rangle_S|0\rangle_E \to C\sqrt{1-p}|1\rangle_S|0\rangle_E + \sqrt{p}|1\rangle_S|2\rangle_E\end{aligned} \tag{22}$$

which means that for an arbitrary state of the qubit $|\psi\rangle_S = C_1|0\rangle_S + C_2|1\rangle_S$, the unitary transformation of the qubit plus environment U_{SE} the total wavefunction is given by

$$\begin{aligned}U_{SE}|\psi\rangle_S|o\rangle_E = C_1|0\rangle_S[\sqrt{1-p}|0\rangle_E+\sqrt{p}|1\rangle_E]\\ +C_2|1\rangle_S[\sqrt{1-p}|0\rangle_E+\sqrt{p}|2\rangle_E]\end{aligned} \tag{23}$$

The Krauss operators of the phase-damping channel can be obtained through evaluating the partial trace over the environment in the $\{|i\rangle_E\}$ basis $M_i =_E \langle i|\hat{U}_{SE}|0\rangle_E$ with the following expressions

$$\begin{aligned}&M_0(p) = \sqrt{1-p}\begin{pmatrix}1&0\\0&1\end{pmatrix},\ M_1(p) = \sqrt{p}\begin{pmatrix}1&0\\0&0\end{pmatrix}\\ &M_2(p) = \sqrt{p}\begin{pmatrix}0&0\\0&1\end{pmatrix}\end{aligned} \tag{24}$$

which satisfy the normalization condition $\sum_{i=0}^{2} M_i = 1$. Therefore, in the depolarizing channel a general initial density matrix ρ of the qubit evolves as

$$\rho' = \begin{pmatrix} \rho_{00} & (1-p)\rho_{01} \\ (1-p)\rho_{10} & \rho_{11} \end{pmatrix} \tag{25}$$

which indicates that thus the on-diagonal terms in ρ remain invariant while the off-diagonal terms decay. The state evolution given by Eq. (25) can be expressed in terms of the Bloch-sphere representation:

$$\begin{aligned} &\rho' = \frac{1}{2}(1 + P' \cdot \hat{\sigma}) \\ &P'_x = (1-p)P_x, \quad P'_y = (1-p)P_y, \quad P'_z = P_z \end{aligned} \tag{26}$$

which indicates that the action of the phase-damping channel is to contract the Bloch sphere to a prolate spheroid about the z-axis. The preferential treatment of the z-direction implies that the phase-damping channel acts in a preferred basis.

3.3 The amplitude-damping channel

In the amplitude-damping channel, the decaying process of the decohring qubit likes the decay of an excited two-level atom due to spontaneous emission of a photon. In this channel, the evolution of the system plus environment is described by a unitary transformation that acts on the system and environment according to

$$\begin{aligned} &|0\rangle_S|0\rangle_E \to |0\rangle_S|0\rangle_E \\ &|1\rangle_S|0\rangle_E \to \sqrt{1-p}|1\rangle_S|0\rangle_E + \sqrt{p}|0\rangle_S|1\rangle_E \end{aligned} \tag{27}$$

which means that for an arbitrary state of the qubit $|\psi\rangle_S = C_1|0\rangle_S + C_2|1\rangle_S$, the unitary transformation of the qubit plus environment U_{SE} the total wavefunction is given by

$$\begin{aligned} U_{SE}|\psi\rangle_S = &C_1|0\rangle_S|0\rangle_E + C_2(\sqrt{1-p}|1\rangle_S|0\rangle_E \\ &+\sqrt{p}|0\rangle_S|1\rangle_E) \end{aligned} \tag{28}$$

The Krauss operators of the amplitude-damping channel can be obtained through evaluating the partial trace over the environment in the $\{|i\rangle_E\}$ basis $M_i = {}_E\langle i|\hat{U}_{SE}|0\rangle_E$ with the following expressions

$$M_0(p) = \begin{pmatrix} 1 & 0 \\ 0 & \sqrt{1-p} \end{pmatrix}, \quad M_1(p) = \begin{pmatrix} 0 & \sqrt{p} \\ 0 & 0 \end{pmatrix} \tag{29}$$

which implies that the state evolution of the system in the amplitude-damping channel is given by

$$\begin{aligned} \rho' &= M_0(p)\rho_i M_0^\dagger(p) + M_1(p)\rho_i M_1^\dagger(p) \\ &= \frac{1}{2}\begin{pmatrix} 1 + P_3 + p(1-P_3) & P_1 - \mathrm{i}P_2\sqrt{(1-p)} \\ \sqrt{(1-p)}(P_1 + \mathrm{i}P_2) & (1-p)(1-P_3) \end{pmatrix} \end{aligned} \tag{30}$$

which leads to the following Bloch-sphere representation of the state evolution:

$$\begin{aligned} &\rho' = \frac{1}{2}(1 + P' \cdot \hat{\sigma}) \\ &P'_x = \sqrt{(1-p)}P_x, \quad P'_y = \sqrt{(1-p)}P_y \\ &P'_z = P_z + p(1-P_z) \end{aligned} \tag{31}$$

which indicates that the action of the amplitude-damping channel is to contract the Bloch sphere to a prolate spheroid about the z-axis. The preferential treatment of the z-direction implies that the amplitude-damping channel acts in a preferred basis.

4 Information-disturbance tradeoff under decoherence

In this section, we study GP quantum repeaters in the presence of decoherence. We evaluate the tradeoff between information gain and quantum state disturbance for quantum repeaters under decoherence through calculating the fidelities of output states of the signal and probe systems with respect to the initial state of the signal system. We explore the possibility of the existence of decoherence-free subspaces for quantum repeaters under decoherence. In order to see these, we consider such a situation in which decoherence occurs only before the signal-probe states enter the quantum repeater indicated in Fig. 3. In other words, quantum states of the signal-probe systems have decohered into mixed states before they enter the quantum repeater due to the effect of their environment. In what follows we will investigate the influence of decoherence on information-disturbance tradeoff of quantum repeaters for three cases of depolarizing damping, phase damping, and amplitude damping, respectively.

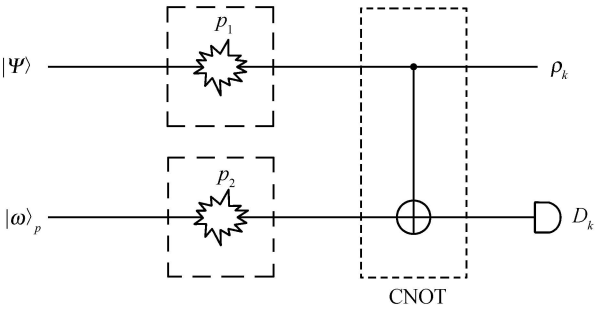

Fig. 3 The schematic diagram of a single-qubit quantum repeater with a single user in the presence of decoherence for the signal qubit and the probe qubit with the decohering parameters p_1 and p_2, respectively.

4.1 The depolarization-damping case

For the depolarization-damping channel, the influence of de-

coherence on quantum states of the signal and probe systems are described by the four Kraus operators defined by Eq. (17). Suppose that the initial states of the signal and probe systems are pure states given by Eqs. (5) and (6), respectively. The initial state is specified by the density matrix $\rho_0 = |\Psi\rangle_s\langle\Psi| \otimes |\omega\rangle_p\langle\omega|$, where s denote the signal mode, and p denote the probe mode. After experiencing decohering processes denoted by the parameters p_1 and p_2, the initial state becomes

$$\rho_1 = \sum_{\mu_s=0}^{3} (M_{\mu_s}|\Psi\rangle_s\langle\Psi|M_{\mu_s}^\dagger) \otimes \sum_{\mu_p=0}^{3} (M_{\mu_p}|\omega\rangle_p\langle\omega|M_{\mu_p}^\dagger) \tag{32}$$

which is the real initial state of the quantum repeater under our consideration. After the CNOT-gate operation denoted by the unitary operator C_{12}, the state denoted by ρ_1 becomes

$$\rho_2 = C_{12}\rho_1 C_{12}^\dagger \tag{33}$$

which is a mixed state of the signal plus probe system.

In order to complete information gain, we have to make σ_z measurements for the probe system. Suppose that $|0\rangle$ and $|1\rangle$ are eigenstates of σ_z with corresponding eigenvalues $+1$ and -1, respectively. We can further assume that after a σ_z measurement of the probe system, the probe is in the state $|0\rangle$ ($|1\rangle$) while the signal is in the normalized state ρ_3 (ρ_4) with the probability P_0 (P_1). Then according to Eqs. (1) and (2), the fidelities F_Ψ and G_Ψ are given by

$$\begin{aligned} F_\Psi &= P_0\langle\Psi|\rho_3|\Psi\rangle + P_1\langle\Psi|\rho_4|\Psi\rangle \\ G_\Psi &= P_0|\langle\Psi|0\rangle|^2 + P_1|\langle\Psi|1\rangle|^2 \end{aligned} \tag{34}$$

where the two normalized states of the signal system are given by the following reduced density operators:

$$\begin{aligned} \rho_3 &= \frac{1}{P_0}[a_{00}|0\rangle\langle 0| + a_{01}|0\rangle\langle 1| + a_{10}|1\rangle\langle 0| + a_{11}|1\rangle\langle 1|] \\ \rho_4 &= \frac{1}{P_1}[b_{00}|0\rangle\langle 0| + b_{01}|0\rangle\langle 1| + b_{10}|1\rangle\langle 0| + b_{11}|1\rangle\langle 1|] \end{aligned} \tag{35}$$

while the two probability functions are defined by

$$P_0 = a_{00} + a_{11}, \quad P_1 = b_{00} + b_{11} \tag{36}$$

where the coefficients a_{ij} are given by

$$\begin{aligned} a_{00} &= \frac{1}{9}\left[3(1-p_1)\cos^2\theta_1 + p_1\sin^2\theta_1 + p_1\right] \\ &\quad \cdot \left[3(1-p_2)\cos^2\theta_2 + p_2\sin^2\theta_2 + p_2\right] \\ a_{11} &= \frac{1}{9}\left[3(1-p_1)\sin^2\theta_1 + p_1\cos^2\theta_1 + p_1\right] \\ &\quad \cdot \left[3(1-p_2)\sin^2\theta_2 + p_2\cos^2\theta_2 + p_2\right] \\ a_{01} &= a_{10}^* = \tfrac{1}{36}\left[(3-4p_1)\mathrm{e}^{-\mathrm{i}\phi_1}\sin(2\theta_1)\right] \\ &\quad \cdot \left[(3-4p_2)\mathrm{e}^{-\mathrm{i}\phi_2}\sin(2\theta_2)\right] \end{aligned} \tag{37}$$

and the coefficients b_{ij} are given by

$$\begin{aligned} b_{00} &= \frac{1}{9}\left[3(1-p_1)\cos^2\theta_1 + p_1\sin^2\theta_1 + p_1\right] \\ &\quad \cdot \left[3(1-p_2)\sin^2\theta_2 + p_2\cos^2\theta_2 + p_2\right] \\ b_{11} &= \frac{1}{9}\left[3(1-p_1)\sin^2\theta_1 + p_1\cos^2\theta_1 + p_1\right] \\ &\quad \cdot \left[3(1-p_2)\cos^2\theta_2 + p_2\sin^2\theta_2 + p_2\right] \\ b_{01} &= b_{10}^* = \frac{1}{36}\left[(3-4p_1)\mathrm{e}^{-\mathrm{i}\phi_1}\sin(2\theta_1)\right] \\ &\quad \cdot \left[(3-4p_2)\mathrm{e}^{\mathrm{i}\phi_2}\sin(2\theta_2)\right] \end{aligned} \tag{38}$$

Then averaging over all the possible input states, i.e., the whole Bloch sphere, we get the transmission fidelity and the estimation fidelity as follows:

$$\begin{aligned} F &= F_0 - \frac{2p_1}{9} - 2D(p_1,p_2)\cos\phi_2\sin(2\theta_2) \\ G &= G_0 - D(p_1,p_2)\cos(2\theta_2) \end{aligned} \tag{39}$$

where we have introduced

$$D(p_1,p_2) = \frac{1}{27}[6(p_1+p_2) - 8p_1p_2] \tag{40}$$

where F_0 and G_0 are the transmission fidelity and the estimation fidelity of the quantum repeater without decoherence, they are given by Eq. (12).

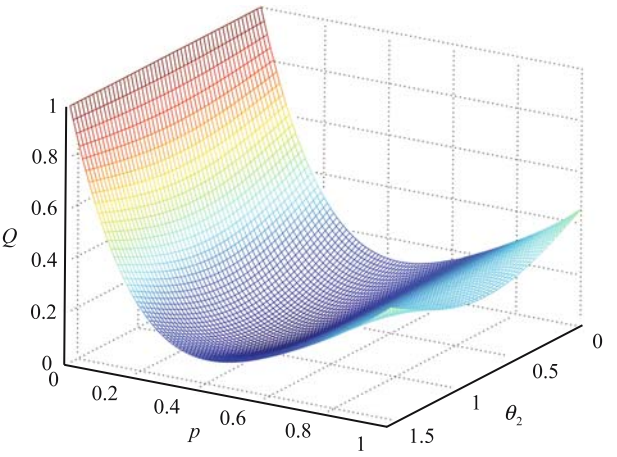

Fig. 4 The quality factor given by Eq. (41) versus the amplitude parameter of the initial probe qubit when $\phi_2 = 0$ and $p_1 = p_2 = p$.

From Eq. (39) we can see that both transmission fidelity and estimation fidelity of the GP quantum repeater are affected by the decoherence, and they can be tuned by chang-

ing the initial-state parameters of the probe qubit θ_2 and ϕ_2, and the damping parameters p_1 and p_2. Obviously, when $p_1 = p_2 = 0$, we have $F = F_0$ and $G = G_0$. This means that we can recover the results when decoherence vanishes.

We now have a look at the influence of decoherence on the optimal character of the quantum repeater. Substituting Eqs. (39) into Eqs. (4) we find the quality factor in the depolarization-damping channel to be

$$Q = \frac{1}{9}[2p_1 - (3 - 18D(p_1, p_2))\sin(2\theta_2)\cos\phi_2]^2 + [1 - 6D(p_1, p_2)]^2\cos^2(2\theta_2) \quad (41)$$

which indicates that when the damping vanishes, i.e., $p_1 = p_2 = 0$, we have $Q = Q_0$. In Fig. 4 we have plotted the quality factor versus the amplitude parameter of the initial probe qubit θ_2 and ϕ_2 and the decohering parameter when $\phi_2 = 0$ and $p_1 = p_2 = p$. From Fig. 4 we can see that decoherence can play different roles in different damping regimes. In the weak damping regime decoherence weakens the optimal character of the quantum repeater while it may enhance the optimal character in the strong damping regime.

In order to better understand the influence of decoherence on information-disturbance tradeoff, for the weak damping (i.e., $p_1 \ll 1$ and $p_2 \ll 1$) we consider the following two cases: (i) $p_1 = p_2 = p$; (ii) $p_1 = 0$ and $p_2 \neq 0$.

In the first case, $p_1 = p_2 = p$, up to the first order of p the transmission fidelity and the estimation fidelity (39) becomes

$$F = F_0 - \frac{2p}{9}[1 + 4\cos\phi_2\sin(2\theta_2)]$$
$$G = G_0 - \frac{4p}{9}\cos(2\theta_2) \quad (42)$$

from which we can see that for the parameter regime of the probe qubit $\{1+4\cos\phi_2\sin(2\theta_2) > 0, \cos(2\theta_2) > 0\}$, which is called as the normal subspace of the probe qubit, we always have $F < F_0$ and $G < G_0$. Hence, decoherence decreases the transmission fidelity and estimation fidelity in the normal subspace. In Fig. 5 we have plotted the trade-off curves between the transmission fidelity and the estimation fidelity in the normal subspace of the probe qubit for the depolarization-damping channel when $\phi_2 = 0, \theta_2 \in (0, \pi/4)$, and $p = 0, 0.02, 0.05$, and 0.1, respectively.

Interestingly, from Eq. (42) we can also find an anomalous subspace $\{1 + 4\cos\phi_2\sin(2\theta_2) < 0, \cos(2\theta_2) < 0\}$ in which we always have $F > F_0$ and $G > G_0$. Therefore, decoherence may enhance the transmission fidelity and estimation fidelity in the anomalous subspace. For instance, let $\theta_2 = 5\pi/8$ and $\phi_2 = 0$ in Eq. (42), we have

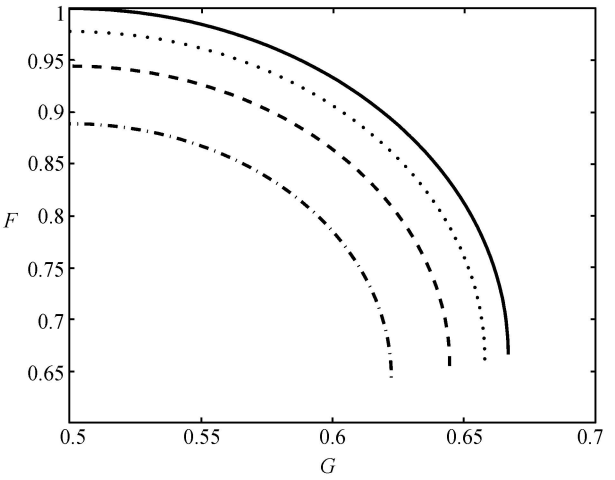

Fig. 5 The trade-off curves between the transmission fidelity and the estimation fidelity in the normal subspace of the probe qubit for the depolarization-damping channel when $\phi_2 = 0$, $\theta_2 \in (0, \pi/4)$, and $p = 0$ (*the solid line*), 0.02 (*the dot line*), 0.05 (*the dashed line*), and 0.1 (*the dot-dashed line*).

$$F = F_0 + \frac{2}{9}(2\sqrt{2} - 1)p > F_0$$
$$G = G_0 + \frac{2\sqrt{2}}{9}p > G_0 \quad (43)$$

In Fig. 6 we have plotted the trade-off curves between the transmission fidelity and the estimation fidelity in the anomalous subspace of the probe qubit for the depolarization-damping channel when $\phi = 2\pi/3$, $\theta_2 \in (\pi/4, \pi/2)$, and $p = 0, 0.02, 0.05$, and 0.1, respectively. Comparing Fig. 6 with Fig. 5 it is easy to see that the trade-off curves between the transmission fidelity and the estimation fidelity exhibit very different characteristics for the normal subspace and the anomalous subspace of the probe qubit. From Fig. 5 it can be seen that the transmission fidelity decreases with the damping parameter p in the normal subspace while the transmission fidelity increases with the damping parameter p in the anomalous subspace for a given value of the estimation fidelity.

In the second case, $p_1 = 0$ and $p_2 \neq 0$, which imply that only the probe qubit experiences decoherence while the signal qubit does not decohere. In this case the transmission fidelity and estimation fidelity (39) becomes

$$F = F_0 - \frac{4}{9}p_2\cos\phi_2\sin(2\theta_2)$$
$$G = G_0 - \frac{2}{9}p_2\cos(2\theta_2) \quad (44)$$

from which we can see that the normal subspace is given by $\{\cos\phi_2\sin(2\theta_2) > 0, \cos(2\theta_2) > 0\}$ in which decoherence decreases the fidelities of the signal and probe qubits due to $F < F_0$ and $G < G_0$ while the anomalous subspace is given

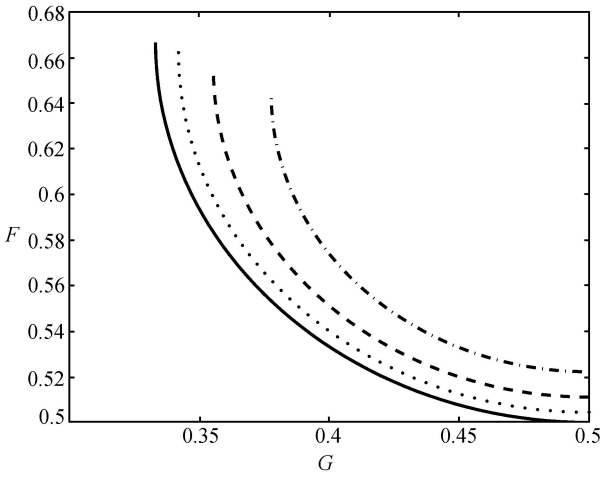

Fig. 6 The trade-off curves between the transmission fidelity and the estimation fidelity in the anomalous subspace of the probe qubit for the depolarization-damping channel when $\phi_2 = 2\pi/3$, $\theta_2 \in (\pi/4, \pi/2)$, and $p = 0$ (*the solid line*), 0.02 (*the dot line*), 0.05 (*the dashed line*), and 0.1 (*the dot-dashed line*).

by $\{\cos\phi_2 \sin(2\theta_2) < 0, \cos(2\theta_2) < 0\}$ in which decoherence enhances the fidelities with $F > F_0$ and $G > G_0$.

From Eq. (44) we can also find that decoherence of the probe qubit does not affect the transmission fidelity and estimation fidelity if we choose initial-state parameters $\theta_2 = (2k+1)\pi/4$ and $\phi_2 = (2k+1)\pi/2$ with k being an integer for the probe qubit, i.e., $F = F_0$ and $G = G_0$. This implies that there exists a DFS of the probe qubit. In the DFS information-disturbance tradeoff does not change under decoherence of the probe qubit.

4.2 The phase-damping-channel case

For the phase-damping channel, the influence of decoherence on quantum states of the signal and probe systems are described by the three Kraus operators defined by Eq. (24). Suppose that the initial states of the signal and probe systems are pure states given by Eqs. (5) and (6), respectively. After experiencing decohering processes denoted by the parameters p_1 and p_2, the initial state becomes

$$\rho_1 = \sum_{\mu_s=0}^{2} (M_{\mu_s} |\Psi\rangle_s \langle\Psi| M_{\mu_s}^\dagger) \otimes \sum_{\mu_p=0}^{2} (M_{\mu_p} |\omega\rangle_p \langle\omega| M_{\mu_p}^\dagger) \tag{45}$$

where $\{M_0, M_1, M_2\}$ are Kraus operators defined by Eq. (24).

Suppose that after a σ_z measurement of the probe system, the probe is in the state $|0\rangle$ ($|1\rangle$) while the signal is in the normalized state ρ_3' (ρ_4') with the probability P_0' (P_1'). Then according to Eqs. (1) and (2), the fidelities F_Ψ' and G_Ψ' are given by

$$\begin{aligned} F_\Psi' &= P_0' \langle\Psi|\rho_3'|\Psi\rangle + P_1' \langle\Psi|\rho_4'|\Psi\rangle \\ G_\Psi' &= P_0' |\langle\Psi|0\rangle|^2 + P_1' |\langle\Psi|1\rangle|^2 \end{aligned} \tag{46}$$

where the two normalized states of the signal system are given by

$$\begin{aligned} \rho_3' &= \frac{1}{P_0'}[c_{00}|0\rangle\langle 0| + c_{01}|0\rangle\langle 1| + c_{10}|1\rangle\langle 0| + c_{11}|1\rangle\langle 1|] \\ \rho_4' &= \frac{1}{P_1'}[d_{00}|0\rangle\langle 0| + d_{01}|0\rangle\langle 1| + d_{10}|1\rangle\langle 0| + d_{11}|1\rangle\langle 1|] \end{aligned} \tag{47}$$

while the two probability functions are defined by

$$P_0' = c_{00} + c_{11}, \quad P_1' = d_{00} + d_{11} \tag{48}$$

where the coefficients c_{ij} and d_{ij} are given by

$$\begin{aligned} c_{00} &= \cos^2\theta_1 \cos^2\theta_2, \quad c_{11} = \sin^2\theta_1 \sin^2\theta_2 \\ c_{01} &= c_{10}^* \\ &= \frac{1}{4}(1-p_1)(1-p_2) e^{-i(\phi_1+\phi_2)} \sin(2\theta_1)\sin(2\theta_2) \\ d_{00} &= \cos^2\theta_1 \sin^2\theta_2, \quad d_{11} = \sin^2\theta_1 \cos^2\theta_2 \\ d_{01} &= d_{10}^* \\ &= \frac{1}{4}(1-p_1)(1-p_2) e^{-i(\phi_1-\phi_2)} \sin(2\theta_1)\sin(2\theta_2) \end{aligned} \tag{49}$$

Then averaging over all the possible input states, i.e., the whole Bloch sphere, we get the transmission fidelity and the estimation fidelity as follows:

$$\begin{aligned} F' &= F_0 - \frac{1}{3}[(p_1+p_2) - p_1 p_2]\cos\phi_2 \sin(2\theta_2) \\ G' &= G_0 \end{aligned} \tag{50}$$

where F_0 and G_0 are the transmission fidelity and the estimation fidelity of the quantum repeater without decoherence, they are given by Eq. (12).

Substituting Eqs. (50) into Eqs. (4) we find the quality factor in the phase-damping channel to be

$$Q' = 1 - \left[1 - (1 - p_1 - p_2 + p_1 p_2)\cos^2\phi_2\right] \sin^2(2\theta_2) \tag{51}$$

which indicates that when the damping vanishes, i.e., $p_1 = p_2 = 0$, we have $Q = Q_0$. It is interesting to note that from Eq. (51) we can see that one can efficiently control and manipulate the quality factor of the quantum repeater by changing the amplitudes and the phase of the probe qubit.

When $\phi_2 = (2k+1)\pi/2$ with k being an integer, we have $Q' = 1 - \sin^2(2\theta_2)$. This means that the quantum repeater can

be immune from the influence of decoherence. In particular, when $\theta_2 = k\pi/2$ with k being an integer, we have $Q' = 1$ which indicates that the quantum repeater becomes an optimal repeater. In Fig. 7 we have plotted the quality factor versus the amplitude parameter of the initial probe qubit θ_2 and ϕ_2 and the decohering parameter when $\phi_2 = 0$ and $p_1 = p_2 = p$.

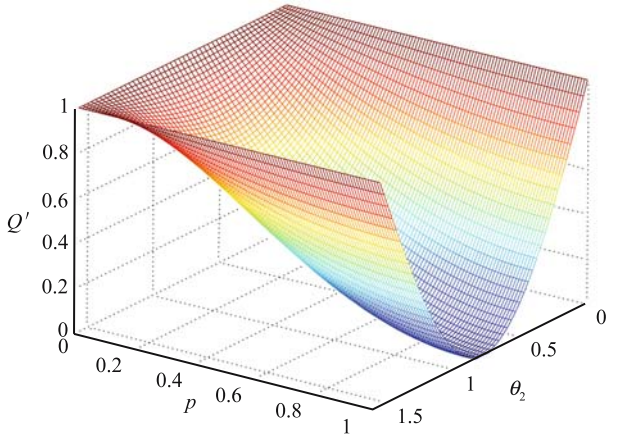

Fig. 7 The quality factor given by Eq. (51) versus the amplitude parameter of the initial probe qubit when $\phi_2 = 0$ and $p_1 = p_2 = p$.

Eq. (50) indicates that the estimation fidelity of the probe qubit is not affected by decoherence in the phase damping channel while decoherence can change the transmission fidelity of the signal qubit. In fact, from Eq. (50) we can see that the normal subspace of the probe qubit is given by the parameter regime of $\{\cos\phi_2 > 0,\ \sin(2\theta_2) > 0\}$ or $\{\cos\phi_2 < 0,\ \sin(2\theta_2) < 0\}$ in which decoherence decreases the transmission fidelity of the signal qubit with $F < F_0$ and $G = G_0$ while the anomalous subspace is given by the parameter regime of $\{\cos\phi_2 > 0,\ \sin(2\theta_2) < 0\}$ or $\{\cos\phi_2 < 0,\ \sin(2\theta_2) > 0\}$ in which decoherence enhances the transmission fidelity with $F > F_0$ and $G = G_0$. It is easy to see that the DFS is given by the parameter regime of $\{\theta_2 = k\pi/2,\ \phi_2 = (2k+1)\pi/2\}$ with k being an integer . In the DFS decoherence does not affect the transmission fidelity, i.e., $F' = F_0$ and $G' = G_0$. In the DFS the information-disturbance tradeoff does not change under decoherence of the probe qubit.

In Fig. 8 we have plotted the trade-off curves between the transmission fidelity and the estimation fidelity in the normal subspace of the probe qubit for the phase-damping channel when $\phi_{=}\pi/4$, $\theta_2 \in (0, \pi/4)$, and $p = 0$ (*the solid line*), 0.1 (*the dot line*), 0.3 (*the dashed line*), and 0.5 (*the dot-dashed line*), respectively. In Fig. 9 we have also plotted the trade-off curves in the anomalous subspace of the probe qubit when $\phi = \pi/4$, $\theta_2 \in (\pi/4, \pi/2)$, and $p = 0$ (*the solid line*), 0.1 (*the dot line*), 0.3 (*the dashed line*), and 0.5 (*the dot-dashed line*), respectively. Comparing Fig. 9 with Fig. 8 it can be seen that the trade-off curves between the transmission fidelity and the estimation fidelity exhibit very different characteristics for the normal subspace and the anomalous subspace of the probe qubit. The transmission fidelity decreases with the damping parameter p in the normal subspace while it increases with the damping parameter p in the anomalous subspace for a given value of the estimation fidelity.

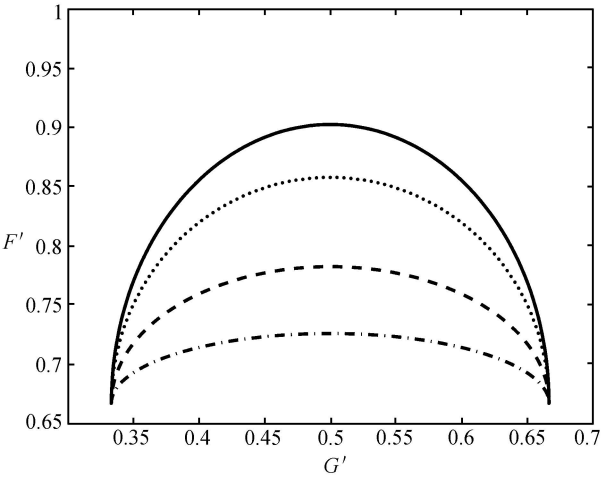

Fig. 8 The trade-off curves between the transmission fidelity and the estimation fidelity in the normal subspace of the probe qubit for the phase damping channel when $\phi = \pi/4$, $\theta_2 \in (0, \pi/4)$, and $p = 0$ (*the solid line*), 0.1 (*the dot line*), 0.3 (*the dashed line*), and 0.5 (*the dot-dashed line*).

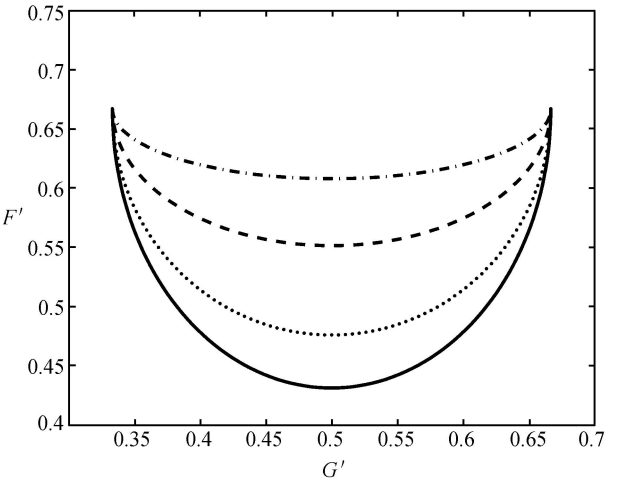

Fig. 9 The trade-off curves between the transmission fidelity and the estimation fidelity in the anomalous subspace of the probe qubit for the phase damping channel when $\phi = 3\pi/4$, $\theta_2 \in (\pi/4, \pi/2)$, and $p = 0$ (*the solid line*), 0.1 (*the dot line*), 0.3 (*the dashed line*), and 0.5 (*the dot-dashed line*).

4.3 The amplitude-damping-channel case

For the amplitude-damping channel, the influence of deco-

herence on quantum states of the signal and probe systems are described by the two Kraus operators defined by Eq. (29). Suppose that the initial states of the signal and probe systems are pure states given by Eqs. (5) and (6), respectively. After experiencing decohering processes denoted by the parameters p_1 and p_2, the initial state becomes

$$\rho_1'' = \sum_{\mu_s=0}^{1} (M_{\mu_s} |\Psi\rangle_s \langle\Psi| M_{\mu_s}^\dagger) \otimes \sum_{\mu_p=0}^{1} (M_{\mu_p} |\omega\rangle_p \langle\omega| M_{\mu_p}^\dagger) \tag{52}$$

where $\{M_0, M_1\}$ are Kraus operators defined by Eq. (29).

Suppose that after a σ_z measurement of the probe system, the probe is in the state $|0\rangle$ ($|1\rangle$) while the signal is in the normalized state ρ_3'' (ρ_4'') with the probability P_0'' (P_1''). Then according to Eqs. (1) and (2), the fidelities F_Ψ'' and G_Ψ'' are given by

$$\begin{aligned} F_\Psi'' &= P_0 \langle\Psi|\rho_3''|\Psi\rangle + P_1 \langle\Psi|\rho_4''|\Psi\rangle \\ G_\Psi'' &= P_0''|\langle\Psi|0\rangle|^2 + P_1''|\langle\Psi|1\rangle|^2 \end{aligned} \tag{53}$$

where the two normalized states of the signal system are given by

$$\begin{aligned} \rho_3'' &= \frac{1}{P_0''}[u_{00}|0\rangle\langle 0| + u_{01}|0\rangle\langle 1| + u_{10}|1\rangle\langle 0| + u_{11}|1\rangle\langle 1|] \\ \rho_4'' &= \frac{1}{P_1''}[v_{00}|0\rangle\langle 0| + v_{01}|0\rangle\langle 1| + v_{10}|1\rangle\langle 0| + v_{11}|1\rangle\langle 1|] \end{aligned} \tag{54}$$

while the two probability functions are defined by

$$P_0'' = u_{00} + u_{11}, \quad P_1'' = v_{00} + v_{11} \tag{55}$$

where the coefficients u_{ij} and v_{ij} are given by

$$\begin{aligned} u_{00} &= [\cos^2\theta_1 + p_1 \sin^2\theta_1][\cos^2\theta_2 + p_2 \sin^2\theta_2] \\ u_{01} &= u_{10}^* \\ &= \frac{1}{4}\sqrt{(1-p_1)(1-p_2)}\mathrm{e}^{-\mathrm{i}(\phi_1+\phi_2)} \sin(2\theta_1)\sin(2\theta_2) \\ u_{11} &= [(1-p_1)\sin^2\theta_1][\cos^2\theta_2 + p_2 \sin^2\theta_2] \\ v_{00} &= [\cos^2\theta_1 + p_1 \sin^2\theta_1][(1-p_2)\sin^2\theta_2] \\ v_{01} &= v_{10}^* \\ &= \frac{1}{4}\sqrt{(1-p_1)(1-p_2)}\mathrm{e}^{-\mathrm{i}(\phi_1-\phi_2)} \sin(2\theta_1)\sin(2\theta_2) \\ v_{11} &= [(1-p_1)\sin^2\theta_1][(1-p_2)\sin^2\theta_2] \end{aligned} \tag{56}$$

Through calculation, we get the transmission fidelity and the estimation fidelity as follows:

$$\begin{aligned} F'' &= \frac{1}{6}(4-p_1) + \frac{1}{3}\sqrt{(1-p_1)(1-p_2)}\cos\phi_2 \sin(2\theta_2) \\ G'' &= \frac{1}{6}(2+p_1+2p_2-2p_1p_2) \\ &\quad + \frac{1}{3}(1-p_1)(1-p_2)\cos^2\theta_2 \end{aligned} \tag{57}$$

where p_1, p_2 are decoherence parameters for the two decohering channels, respectively. For the situation of $p_1 = p_2 = p$, Eq. (57) becomes the following simple expression:

$$\begin{aligned} F'' &= \frac{1}{6}(4-p) + \frac{1}{3}(1-p)\cos\phi_2 \sin(2\theta_2) \\ G'' &= \frac{1}{6}(2+3p-2p^2) + \frac{1}{3}(1-p)^2\cos^2\theta_2 \end{aligned} \tag{58}$$

Substituting Eqs. (58) into Eqs. (4) we find the quality factor in the amplitude-damping channel to be

$$\begin{aligned} Q'' &= \frac{1}{4}[p - 2(1-p)\cos\phi_2 \sin(2\theta_2)]^2 \\ &\quad + [p(1-p) + (1-p)^2\cos^2(2\theta_2)]^2 \end{aligned} \tag{59}$$

which indicates that when the damping vanishes, i.e., $p_1 = p_2 = 0$, we have $Q = Q_0$. In Fig. 6 we have plotted the quality factor versus the amplitude parameter of the initial probe qubit θ_2 and ϕ_2 and the decohering parameter when $\phi_2 = 0$ and $p_1 = p_2 = p$. From Fig. 4 we can see that decoherence weakens the optimal character of the quantum repeater.

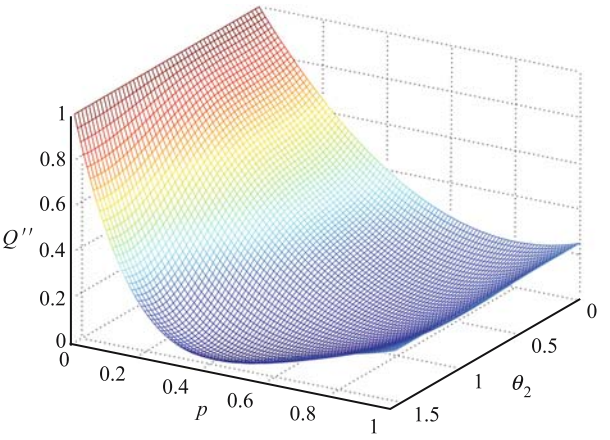

Fig. 10 The quality factor given by Eq. (59) versus the amplitude parameter of the initial probe qubit when $\phi_2 = 0$ and $p_1 = p_2 = p$.

In the regime of weak damping $p_1 \ll 1$ and $p_2 \ll 1$, up to the first order to the damping parameters p_1 and p_2 the transmission fidelity and the estimation fidelity become

$$\begin{aligned} F'' &= F_0 - \frac{p_1}{6} - \frac{1}{6}(p_1+p_2)\cos\phi_2 \sin(2\theta_2) \\ G'' &= G_0 + \frac{1}{6}(p_1+2p_2) - \frac{1}{3}(p_1+p_2)\cos^2\theta_2 \end{aligned} \tag{60}$$

which indicates that if the signal qubit and the probe qubit have the same damping parameters, say $p_1 = p_2 = p$, from

Eq. (60) we have

$$F'' = F_0 - \frac{p}{6}[1 + 2\cos\phi_2 \sin(2\theta_2)]$$
$$G'' = G_0 + \frac{p}{6}(3 - 4\cos^2\theta_2) \quad (61)$$

which indicate that both of the transmission fidelity and the estimation fidelity is dependent of the decoherence parameter. However, for the estimation fidelity of the probe qubit, the normal subspace is given by the parameter regime of $\{1 + 2\cos\phi_2 \sin(2\theta_2) < 0, \cos^2\theta_2 > 3/4\}$ while the anomalous subspace is given by the parameter regime of $\{1 + 2\cos\phi_2 \sin(2\theta_2) > 0, \cos^2\theta_2 < 3/4\}$. In particular, when we choose initial-state parameters $\cos^2(\theta_2) = 3/4$ and $\cos\phi_2 = -1/[2\sin(2\theta_2)]$ for the probe qubit, we obtain $F'' = F_0$ and $G'' = G_0$. This implies that there exists a DFS of the probe qubit.

Finally, in order to see the similar or/and different characteristics of the quality factor and fidelities for different damping channels. In Fig. 11 we have plotted the quality factor versus the damping parameter for three types of damping channels when the initial parameters of the probe qubit are $\phi_2 = 0$ and $\theta_2 = \pi/4$. From Fig. 11 we can see that the quality factor of the quantum repeater may exhibit different characteristics in different damping regimes. For instance,in the weak damping regime the quality factor decreases with the damping parameter p for the three damping channels, and the amplitude-damping channel has the best quality factor while the depolarization-damping channel has the worst quality factor. However, in the strong damping regime the quality factor increases with the damping parameter p for the amplitude and depolarization damping channels, and the depolarization-damping channel has the best quality factor.

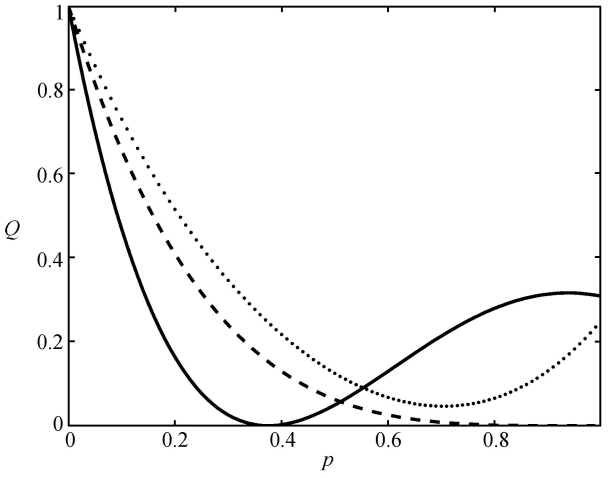

Fig. 11 The influence of damping on the quality factor of the quantum repeater when the initial parameters $\phi_2 = 0$ and $\theta_2 = \pi/4$ for three types of damping channels: the depolarization-damping channel (*the solid line*), the phase-damping channel (*the dashed line*), and the amplitude damping channel (*the dot line*).

In Fig. 12 we have plotted the trade-off curves between the transmission fidelity and the estimation fidelity for three types of damping channels when $\phi_2 = 0, p_1 = p_2 = p = 0.1$ and 0.3 in Fig. 3, respectively. From Fig. 3 we can see that for three channels the larger the decoherence parameter p, the further the resulting trade-off curves from the bound (*the solid line*). This means that the decoherence can decrease the information acquirement for users. We can also see that the decohering influence of the phase-damping channel and the amplitude-damping channel on the trade off is smaller than that of the depolarizing channel. The trade-off is most sensitive to decoherence induced by the depolarization damping channel.

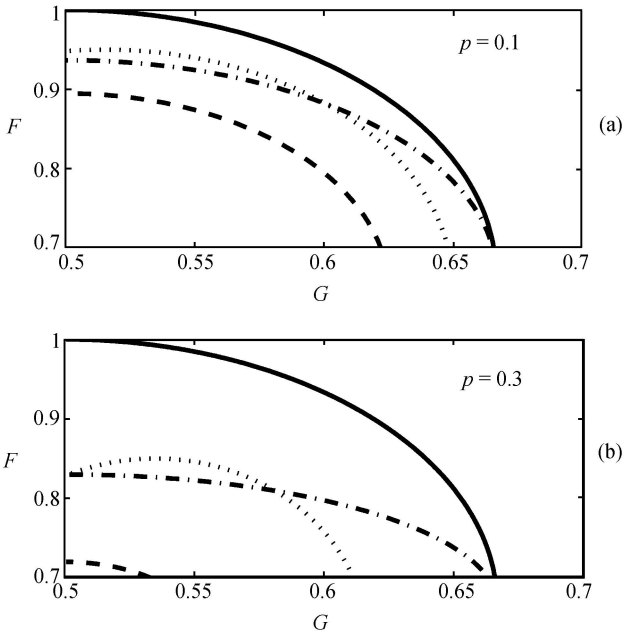

Fig. 12 The trade-off curves between the transmission fidelity and the estimation fidelity for three types of damping channels when the damping parameter $p = 0.1$ **(a)** and 0.3 **(b)**, respectively. The solid line denotes the curve of $F_0(G_0)$ without decoherence. The dot-dashed lines denote $F(G)$ for the phase damping channel, dotted lines denote $F(G)$ for the amplitude damping channel, and the dashed lines denote $F(G)$ for the depolarizing channel.

5 Concluding remarks

In this paper, we have studied single-qubit and single-user quantum repeaters based on a CNOT gate under decoherence in terms of the Kruas-operator representations of deco-

herence by calculating the transmission fidelity and the estimation fidelity for the signal qubit and the probe qubit, respectively. We have investigated the influence of decoherence on the information-disturbance trade-off of quantum repeaters by calculating the transmission fidelity and the estimation fidelity for the signal qubit and the probe qubit, respectively. Three types of damping channels, i.e., the depolarizing channel, the phase-damping channel, and the amplitude-damping channel are discussed in detail. It has been found that decoherence may lead to the appearance of three subspaces, i.e., the normal subspace, the anomalous subspace, and the DFS. It has been shown that in different subspaces of the probe qubit, the transmission fidelity and the estimation fidelity of the GP quantum repeaters exhibit different characteristics. In the normal subspace the presence of decoherence decreases the transmission fidelity and the estimation fidelity while these fidelities may be enhanced in the anomalous subspace. However, in the DFS, these fidelities do not change. Hence, in the DFS decoherence does not affect the information-disturbance trade-off of quantum repeaters.

We have analytically and numerically investigated the trade-off between the information gain and quantum state disturbance for the GP quantum repeater through calculating the transmission fidelity and the estimation fidelity. It has been shown that the trade-off between the transmission fidelity and the estimation fidelity exhibits different sensibility to different damping channels and different damping regimes in the same damping channel. The trade-off is most sensitive to decoherence induced by the depolarization-damping channel. We have introduced the concept of the quality factor to evaluate the quality of the quantum repeater. It has been indicated that decoherence can play different roles in different damping regimes, and the quality factor can be efficiently controlled and manipulated by changing the amplitudes and the phase of the probe qubit. It has been found that under certain conditions the quantum repeater can be immune from the influence of decoherence for the depolarization-damping channel. This means that under these conditions the quantum repeater is optimal even in the presence of decoherence. It should be mentioned that in the present paper we only consider decoherence of the signal and probe systems before carrying out the CNOT operation. In fact, both of the incompleteness of the CNOT operation and the evolution after the CNOT operation may produce further decohering processes. These are interesting problems deserved to be further studied.

Acknowledgements This work was supported by the National Fundamental Research Program under Grant No. 2007CB925204, by the National Natural Science Foundation under Grant Nos. 10325523, by the Foundation of the Education Ministry of China, and by the Education Committee of Hunan Province.

References

1. Briegel H. J., Dür W., Cirac J. I., and Zoller P., Phys. Rev. Lett., 1998, 81: 5932
2. Boozer A. D., Boca A., Miller R., Northup T. E., and Kimble H. J., Phys. Rev. Lett., 2007, 98: 193601
3. Simon C., de Riedmatten H., fzelius M., Sangouard N., Zbinden H., and Gisin N., Phys. Rev. Lett., 2007, 98: 190503
4. Yuan Z. S., Chen Y. A., Chen S., Zhao B., Koch M., Strassel T., Zhao Y., Zhu G. J., Schmiedmayer J., and Pan J. W., Phys. Rev. Lett., 2007, 98: 180503
5. Collins O. A., Jenkins S. D., Kuzmich A., and Kennedy T. A., Phys. Rev. Lett., 2007, 98: 060502
6. Hartmann L., Kraus B., Briegel H.-J., and Dür W., Phys. Rev. A, 2007, 75: 032310
7. Loock P. van, Ladd T. D., Sanaka K., Yamaguchi F., Nemoto K., Munro W. J., and Yamamoto Y., Phys. Rev. Lett., 2006, 96: 240501
8. Chen Y. A., Zhang A. N., Zhao Z., Zhou X. Q., and Pan J. W., Phys. Rev. Lett., 2006, 96: 220504
9. Pan J. W., Gasparoni S., Ursin R., Weihs G., and Zeilinger A., Nature (London), 2003, 423: 417
10. Dür W. and Briegel H. J., Rep. Prog. Phys., 2007, 70: 1381
11. Gisin N., Ribordy G., Tittel W., and Zbinden H. O., Rev. Mod. Phys., 2002, 74: 145
12. Klein A., Dorner U., Alves C. M., and Jaksch D., Phys. Rev. A, 2006, 73: 012332
13. ChildressL., Taylor J. M., Sørensen A. S., and Lukin M. D., Phys. Rev. A, 2005, 72: 052330
14. Hutton A. and Bose S., Phys. Rev. A, 2002, 65: 022321
15. Kok P., Williams C. P., and Dowling J. P., Phys. Rev. A, 2003, 68: 022301
16. Braginsky V. B. and Khalili F. Y., Quantum Measurement, Cambridge: Cambridge University Press, 1992
17. Namiki N., Pascazio S., and Nakazato H., Decoherence and Quantum Measurements, Singapore: World Scientific, 1997
18. Sun C. P. and Yu L. H., Phys. Rev. A, 1995, 51: 1845
19. Liu X. F. and Sun C. P., Phys. Lett. A, 1995, 198: 371
20. Sun C. P., Liu X. F., Zhou D. L., and Yu S. X., Phys. Rev. A, 2000, 63: 012111
21. Sun C. P., Liu X. F., Zhou D. L., and Yu S. X., Phys. Rev. A, 2000, 63: 012111
22. Sun C. P., Phys. Rev. E, 1993, 48: 898
23. Sun C. P., Yi X. X., and Liu X. F., Fortschr. Phys., 1995, 43: 585
24. Zhang P., Liu X. F., and Sun C. P., Phys. Rev. A, 2002, 66: 042104
25. Zhou D. L., Zhang P., and Sun C. P., Phys. Rev. A, 2002, 66: 012112
26. Sciarrino F., Ricci M., De Martini F., Filip R., and Mišta L., Jr., Phys. Rev. Lett., 2006, 96: 020408
27. Scully M. O., Englert B.-G., and Walther H., Nature (London), 1991, 351: 111
28. Dürr S., Nonn T., and Rempe G., Nature (London), 1998, 395: 33
29. Bertet P., et al., Nature (London), 2001, 411: 166

30. Englert B. G., Phys. Rev. Lett., 1996, 77: 2154
31. Ekert A. K., Huttner B., Palma G. M., and Peres A., Phys. Rev. A, 1994, 50: 1047
32. Fuchs C. A. and Peres A., Phys. Rev. A, 1996, 53: 2038
33. Biham E. and Mor T., Phys. Rev. Lett., 1997, 78: 2256
34. Lütkenhaus N., Phys. Rev. A, 1999, 59: 3301
35. Bechmann-Pasquinucci H. and Gisin N., Phys. Rev. A, 1999, 59: 4238
36. Banaszek K., Phys. Rev. Lett., 2001, 86: 1366
37. Sacchi M. F., Phys. Rev. Lett., 2006, 96: 220502
38. Maccone L., Phys. Rev. A, 2006, 73: 042307
39. Mišta L., Phys. Rev. A, 2006, 73: 032335
40. Sciarrino F., Ricci M., De Martini F., Filip R., and Mitša L., Phys. Rev. Lett., 2006, 96: 020408
41. Andersen U. L., Sabuncu M., Filip R., and Leuchs G., Phys. Rev. Lett., 2006, 96: 020409
42. Mišta L. and Filip R., Phys. Rev. A, 2005, 72: 034307
43. Li L. and Chen Z. B., Phys. Rev. A, 2005, 72: 014302
44. Banaszek K. and Devetak I., Phys. Rev. A, 2001, 64: 052307
45. Zhang S. L., Zou X. B., Li K., Jin C. H., and Guo G. C., Chin. Phys. Lett., 2007, 24: 1456
46. Zurek W. H., Phys. Today, 1991, 44: 36
47. Chuang I. L., Laflamme R, Shor P. W., and Zurek W. H., Science, 1991, 270: 1633
48. Sun C. P., Zhan H., and Liu X. F., Phys. Rev. A, 1998, 58: 1810
49. Sun C. P., Gao Y. B., Dong H. F., and Zhao S. R., Phys. Rev. E, 1998, 57: 3900
50. Kuang L. M., Tong Z. Y., Ouyang Z. W., and Zeng H. S., Phys. Rev. A, 1999,61: 013608
51. Kuang L. M., Zeng H. S., and Tong Z. Y., Phys. Rev. A, 1999, 60: 3815
52. Kuang L. M., Chen X, Chen G. H., and Ge M. L., Phys. Rev. A, 1997, 56: 3139
53. Sun Y. H., Zhu X., and Kuang L. M., Chin. Phys. Lett., 2005, 22: 1833
54. Tong Z. Y. and Kuang L. M., Chin. Phys. Lett., 2006, 23: 1076
55. Zeng A. H. and Kuang L. M., Commun. Theor. Phys., 2004, 41: 41
56. Shor P. W., Phys. Rev. A, 1995, 52: R2493
57. Steane A. M., Phys. Rev. Lett., 1996, 77: 793
58. Ekert A. and Macchiavello C., Phys. Rev. Lett., 1996, 77: 2585
59. Knill E., Laflamme R., and Zurek W. H., Science, 1998, 279: 342
60. Raussendorf R. and Harrington J., Phys. Rev. Lett., 2007, 98: 190504
61. DiVincenzo D. P. and Aliferis P., Phys. Rev. Lett., 2007, 98: 020501
62. Aharonov D., Kitaev A., and Preskill J., Phys. Rev. Lett., 2006, 96: 050504
63. Kielpinski D., Meyer V., Rowe M. A., Sackett C. A., Itano W. M., Monroe C., and Wineland D. J., Science, 2001, 291: 1013
64. Langer C., Ozeri R., Jost J. D., Chiaverini J., DeMarco B., Ben-Kish A., Blakestad R. B., Britton J., Hume D. B., Itano W. M., Leibfried D., , Reichle R., Rosenband T., Schaetz T., Schmidt P. O., and Wineland D. J., Phys. Rev. Lett., 2005, 95: 060502
65. Ollerenshaw J. E., Lidar D. A., and Kay L. E., Phys. Rev. Lett., 2003, 91: 217904
66. Viola L., Fortunato E. M., Pravia M. A., Knill E., Laflamme R., and CoryD. G., Science, 2001, 293: 2059
67. Kwiat P. G., Berglund A. J., Altepeter J. B., and White A. G., Science, 2000, 290: 498
68. Bourennane M., Eibl M., Gaertner S., Kurtsiefer C., Cabello A., and Weinfurter H., Phys. Rev. Lett., 2004, 92: 107901
69. Genoni M. G. and Paris M. G. A., Phys. Rev. A, 2005, 71: 052307
70. Genoni M. G. and Paris M. G. A., J. Phys. Conference Series, 2007, 67: 012029
71. Preskill J., Caltech Lecture Notes, http:// www.theorycaltech. edu/ preskill/ph229
72. Nielsen M. A. and Chuang I. L., Quantum Computation and Quantum Information, Cambridge: Cambridge University Press, 2000
73. Kraus K., State, Effects and Operations, Berlin: Springer, 1983
74. Liu Y. X., Özdemir S. K., Miranowicz A., and Imoto N., Phys. Rev. A, 2004, 70: 042308
75. Chen J. L. and Oh L. C., Phys. Rev. A, 2002, 65: 052320
76. Zhu X. and Kuang L. M., J. Phys. A: Math. Theor., 2007, 40: 7729